Organic Electronics 13 (2012) 1261–1265

Contents lists available at SciVerse ScienceDirect

Organic Electronics

journal homepage: www.elsevier.com/locate/orgel

Effect of organic spacer in an organic spin valve using organic magnetic semiconductor $V[TCNE]_x$

Bin Li [a], Mengqi Zhou [b], Yu Lu [b], Chi-Yueh Kao [b], Jung-Woo Yoo [c], Vladimir N. Prigodin [a,d], Arthur J. Epstein [a,b,*]

[a] Department of Physics, The Ohio State University, Columbus, OH 43210-1117, USA
[b] Department of Chemistry, The Ohio State University, Columbus, OH 43210-1173, USA
[c] School of Mechanical and Advanced Materials Engineering, UNIST, Ulsan 689-798, Republic of Korea
[d] Ioffe Institute, St. Petersburg 194021, Russia

ARTICLE INFO

Article history:
Received 3 January 2012
Received in revised form 19 March 2012
Accepted 24 March 2012
Available online 17 April 2012

Keywords:
Magnetoresistance
Spin valve
Organic-based magnet
Organic semiconductor
Organic spintronics

ABSTRACT

We studied the role of organic semiconductor spacer tris (8-hydroxyquinoline) (Alq_3) in a hybrid spin valve which is comprised of $V[TCNE]_x$ ($x \sim 2$, TCNE: tetracyanoethylene) and Fe as the ferromagnetic layers. We compare two types of devices: Fe/$V[TCNE]_x$/Al and Fe/Alq_3/$V[TCNE]_x$/Al, showing that organic spacer is not indispensable for the appearance of the spin valve effect. However, the device with Alq_3 spacer has magnetoresistance (MR) value one order of magnitude larger than the device without spacer. The MR of both devices diminish with increasing temperature, while only the Fe/Alq_3/$V[TCNE]_x$/Al device shows room-temperature MR.

1. Introduction

Spintronics is spin-based electronics which explores the spin degree of freedom in order to convey information encoded with spin states, adding new dimension of functionality to the conventional semiconductor charge-based electronics [1]. The merging of organic electronics and spintronics gives rise to the new field of organic spintronics [2,3]. The long spin-relaxation time in carbon-based systems due to small spin–orbit coupling and weak hyperfine interaction is of great interests. In spite of the long spin-relaxation time, the spin diffusion length is limited by the low carrier mobilities in organic materials [4]. Thus efforts of studying spin injection/detection have been focused on vertical spin valve devices. In a vertical tri-layer FM/NM/FM spin valve structure, a non-magnetic spacer is used to decouple the two ferromagnetic layers. Then, the two magnetic layers can have parallel and antiparallel alignments of the magnetization depending on external magnetic field, leading to different resistance values for each alignment. Several organic semiconductors have been used to act as the spacer in tri-layer spin valve structure, including tris (8-hydroxyquinoline)-aluminum (Alq_3) [5–10], rubrene [11–17], and fullerence C_{60} [18,19]. In these spin valve devices, though the organic spacer has thickness larger than the tunneling limit, roughness of organic semiconductor and their high resistance make these device can be regarded as magnetic tunneling junctions. In general, spin injection from ferromagnetic metals into semiconductor is still challenging, in part due to the 'conductivity mismatch' problem [20]. The use of organic-based magnet as the magnetic contact provides an alternative way to solve this problem [21]. Here we report our studies of the effect of organic spacer on the performance of an organic spin valve based on organic magnetic semiconductor vanadium tetracyanoethylene ($V[TCNE]_x$, $x \sim 2$). We observed spin valve effect in devices without

* Corresponding author at: Department of Physics, The Ohio State University, Columbus, OH 43210-1117, USA. Tel.: +1 (614) 292 1133; fax: +1 (614) 292-7557.
E-mail address: epstein@physics.osu.edu (A.J. Epstein).

1566-1199/$ - see front matter © 2012 Elsevier B.V. All rights reserved.
http://dx.doi.org/10.1016/j.orgel.2012.03.038

non-magnetic spacer and show that the introduction of organic spacer greatly improved the MR value of the devices.

V[TCNE]$_x$ is the first reported room temperature organic-based magnet with magnetic ordering temperature $T_c \sim 400$ K [22]. The V^{2+} ion's three unpaired electrons in $3d(t_{2g})$ orbitals are antiferromagnetically coupled to the $[TCNE]^-$ anion's unpaired electron in π^* orbital, leading to a net spin S = 1/2 for the repeat unit [23]. V[TCNE]$_x$ can be grown as a thin film by low-temperature (~40°C) chemical vapor deposition (CVD) or molecular layer deposition (MLD) [24,25]. Extended X-ray absorption fine structure (EXAFS) analysis showed that each vanadium ion is coordinated by six nitrogen atoms at an average distance of 2.084(5) Å[26]. V[TCNE]$_x$ has a unique half-semiconductor electronic structure with fully spin-polarized valence and conduction bands [23].We have reported hybrid spin valve as well as all-organic-based spin valve, successfully demonstrated spin injection/detection using organic-based magnet [13,16]. Optical detection of spin injection from organic-based magnet into GaAs quantum well is also realized [27].

2. Materials and methods

Detail description of the device fabrication procedure is discussed in earlier publication [17]. The bottom Fe contact and the organic spacers were thermally evaporated in two high-vacuum deposition chambers separately (base pressure: 10^{-7} Torr) inside of an argon-filled glovebox, onto pre-cleaned glass substrates using shadow masks. 300 nm of V[TCNE]$_x$ films grown by CVD were used for the second ferromagnetic layers. Finally, the devices were capped by 30 nm of Al top electrode. The device area is around 1 mm × 1 mm, defined by a cross-bar structure. We fabricated and compared two types of devices with the device structures of Fe (50 nm)/V[TCNE]$_x$ (300 nm)/Al (30 nm), Fe (50 nm)/Alq_3 (10 nm)/V[TCNE]$_x$ (300 nm)/Al (30 nm). We also compared the results from previous report on Fe (50 nm)/rubrene (10 nm)/V[TCNE]$_x$ (300 nm)/Al (30 nm) [17]. All the electrical and magneto transport measurements were performed in a physical property measurement system (PPMS) from Quantum Design. After the device fabrication in the argon glovebox, the samples were immediately transferred to PPMS using an argon-filled protective package, to minimize the air exposure.

3. Results

3.1. Fe/V[TCNE]$_x$/Al structure

Fig. 1 shows the current–voltage (I–V) characteristics of the device with the structure of Fe (50 nm)/V[TCNE]$_x$ (300 nm)/Al (30 nm) at different temperatures. The I–V curves are non-linear and strongly temperature-dependent. As discussed in previous literature [6,11], the appearance of zero bias anomalies in the conductance vs bias plot is mostly due to the metallic interdiffusion through the barrier and the absence of zero bias dips usually indicates the quality of the tunnel barrier. Here we prevent this metallic interdiffusion problem by employing organic-

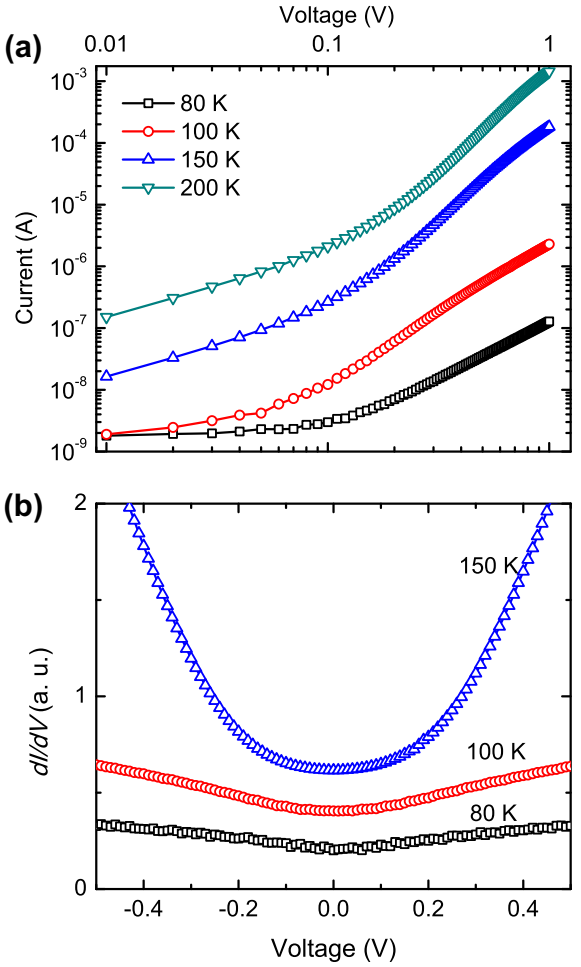

Fig. 1. (a) I–V characteristics of the device with the structure of Fe/V[TCNE]$_x$/Al) at different temperatures: 80 K, 100 K, 150 K and 200 K. (b) dI/dV at different temperatures: 80 K, 100 K and 150 K.

based magnet grown by low temperature CVD. Fig. 2 displays the magnetoresistance (MR) measurements results of the Fe/V[TCNE]$_x$/Al device. Fig. 2(a) shows three MR curves recorded at a bias voltage of 1000 mV at different temperatures: 80 K, 100 K and 150 K. The higher coercive field is attributed to Fe and V[TCNE]$_x$ film has a smaller coercivity of 4.5 Oe at 100 K. The MR value is defined as: $MR = (R_{AP} - R_P)/R_P \times 100\%$, where R_{AP} and RP are the device resistances corresponding to antiparallel and parallel configurations respectively. At 80 K, the value of MR is 0.11% and continuously decreases as T increases (Fig. 2(b)). MR disappeared as T was increased over 200 K. The plot of MR as a function of the applied bias is displayed in Fig. 2(b). The MR value increases as the bias voltage is raised, and reached to a value of 0.11% at a bias voltage of 3000 mV. We did not apply bias voltages higher that 3000 mV to avoid device break down.

3.2. Fe/Alq_3/V[TCNE]$_x$/Al structure

Fig. 3 shows the I–V curves of the device with 10 nm Alq_3 spacer at different temperatures: 80 K, 100 K, 150 K, and

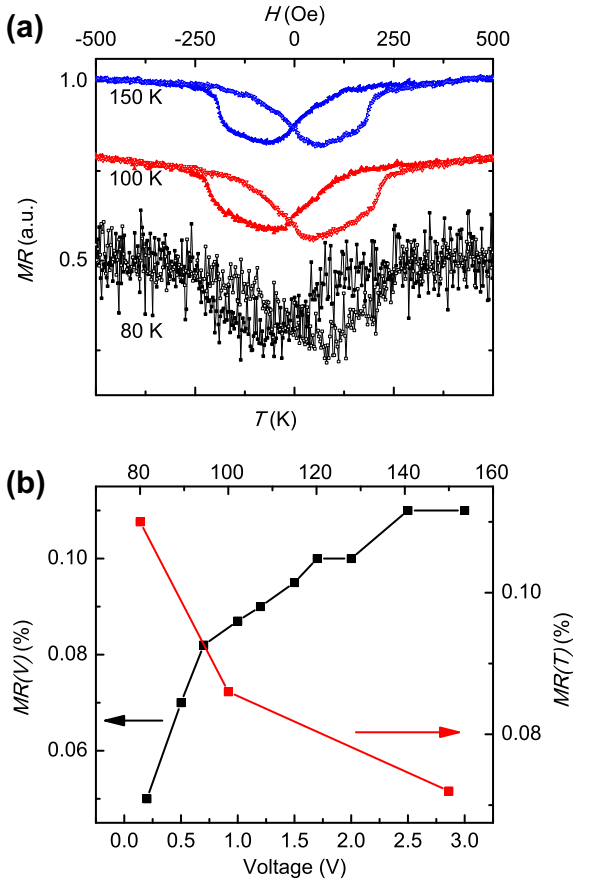

Fig. 2. (a) Magnetoresistance (MR) curves of the device with the structure of Fe/V[TCNE]$_x$/Al) at different temperatures: 80 K, 100 K, and 150 K at a bias voltage of 1000 mV. (b) Bias dependence (black) of MR values at 100 K and temperature dependence (red) of MR values at 1000 mV. (For interpretation of the references to colour in this figure legend, the reader is referred to the web version of this article.)

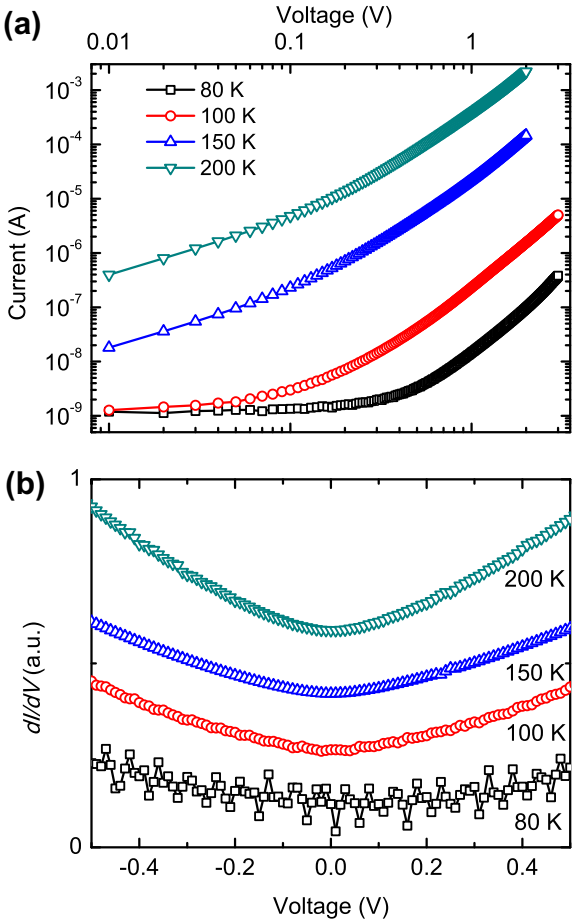

Fig. 3. (a) *I–V* characteristics of the device with the structure of Fe/Alq$_3$/V[TCNE]$_x$/Al at different temperatures: 80 K, 100 K, 150 K and 200 K. (b) *dI/dV* at different temperatures: 80 K, 100 K, 150 K and 200 K.

200 K. The *I–V* curves are also non-linear and strongly temperature dependent. The absence of zero bias anomalies in the *dI/dV* vs bias plots implies the Alq$_3$ forms a good tunnel barrier. Fig. 4 presents MR curves of the Fe/Alq$_3$/V[TCNE]$_x$/Al device at different temperatures range from 100 K to 300 K. The MR of the devices decreases as the temperature increases, which is typical behavior of magnetic tunnel junction [6,11]. At a bias voltage of 500 mV, the MR decreases from 0.32% at 100 K to 0.05% at 300 K. Note that we also realized room-temperature spin injection/detection in this system, as we reported before using rubrene as the spacer [17]. Compared to the Fe/V[TCNE]$_x$/Al device, the device with Alq$_3$ spacer shows a different bias dependence of MR values (see Fig. 5(a)). As applied bias voltage increases, the MR value decreases, which is typical behavior of magnetic tunnel junction. The opposite bias dependence of the previous device might be due to the fact that voltage drop in that device occurs mostly through the bulk of V[TCNE]$_x$ rather than the tunnel barrier. At 150 K, we obtained a MR of 0.7% at 10 mV and the MR decreased to 0.09% at 2000 mV. Fig. 5(b) displays the recorded MR curves at 150 K at different bias voltages. Compared to the MR curves of the device without spacer, the Fe/Alq$_3$/V[TCNE]$_x$/Al device shows more sharp and distinct switch at the coercive fields of the ferromagnetic layers. We also measured the device resistance as a function of temperature. As shown in Fig. 6, the resistances of both devices increased by several orders of magnitude as we lowered the temperature from 300 K to around 60 K. In the device without barrier, the activation is mostly due to the bulk of V[TCNE]$_x$. The device with Alq$_3$ spacer displays stronger temperature dependence reflecting the presence of activation barrier between two ferromagnetic layers.

4. Discussion

Previously, one of the difficulties in device fabrication is to eliminate pinholes. When ferromagnetic metals are deposited onto soft organic spacer layer, hot metal atoms would penetrate into the organic layer and form filamentary pinholes [14]. One of the advantages of using organic-based magnet is the low temperature deposition process which avoids the penetration of metal atoms. The

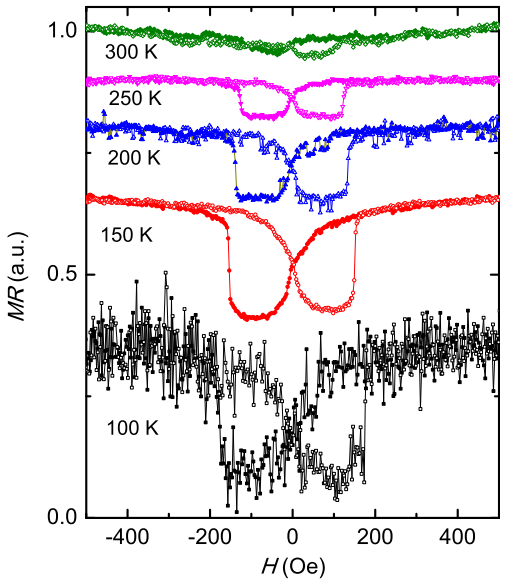

Fig. 4. Magnetoresistance (MR) curves of the device with the structure of Fe/Alq_3/V[TCNE]$_x$/Al recorded at 500 mV at different temperature: (from bottom to top) 100 K, 150 K, 200 K, 250 K and 300 K.

temperature-dependent non-linear *I–V* curves as well as the semiconductor-like temperature-dependent device resistance imply that our devices are free of pinholes. Particularly, as Åkerman et al. suggested [28], examining temperature dependence of the resistance is a reliable way to rule out pinholes through the barrier. As shown in Fig. 6, the slope of the Fe/Alq_3/V[TCNE]$_x$/Al device is larger than that of the device without Alq_3 spacer, indicating the resistance of the former increases more rapidly as the temperature decreases. This could be attributed to the presence of activation barrier between the two ferromagnetic layers.

As reported previously [23,29], the resistance of V[TCNE]$_x$ increases linearly with increasing magnetic field, centering at zero field without any shift. The MR from V[TCNE]$_x$ is at least one order of magnitude smaller than the MR we obtained in our multilayer junctions. Thus the MR in our devices should come from spin valve effect. By making two ferromagnetic layers directly contacting each other, one may expect the exchange interaction between them would hinder free rotation of the magnetization vectors in the absence of a spacer to decouple the two contacts. However, in our experiments, the device without Alq_3 spacer shows distinct MR up to 200 K. One possible reason accounting for this discrepancy is the existence of a thin Fe oxide layer on top of deposited Fe film. Even though the Fe deposition and following CVD process were performed in an argon-filled glovebox without the sample's exposure to air, the metallic film cannot be guaranteed to be free of oxidation. Another possibility is the formed 'dead layer' due to chemical reaction between the V[TCNE]$_x$ and Fe, similar with the 'ill-defined layer' proposed by Xiong et al. in the report of the first vertical organic spin valve [5]. Careful probe and analysis of the interface between the V[TCNE]$_x$ and Fe would be helpful to confirm this possibility. However, due to the air sensitivity of the V[TCNE]$_x$ film, we do not have access to this interface at this moment. Future advancement of film depositin technique and property-controlling methods might shed light on this issue.

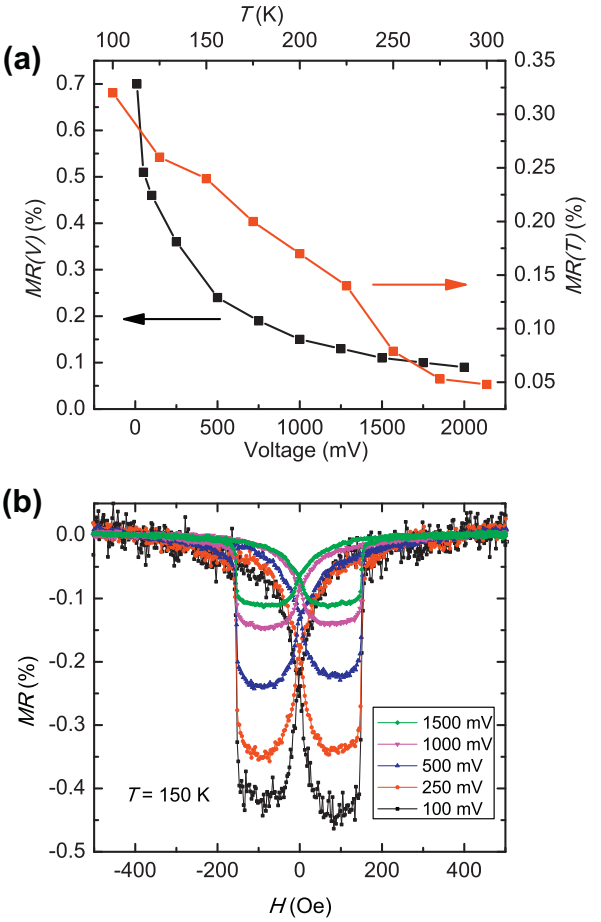

Fig. 5. (a) Temperature dependence (red) of MR values of the device with the structure of Fe/Alq_3/V[TCNE]$_x$/Al at a bias voltage of 500 mV. Bias voltage dependence (black) of MR values at 150 K. (b) MR curves recorded at 150 K at different bias voltages range from 100 mV to 1500 mV.

Both the two types of devices show smaller MR value at higher temperature. This temperature dependence is common in reported magnetic tunnel junctions and explained by the temperature dependence of the defect density in the barrier [11]. Interestingly, the two types of devices have different bias dependence of MR values. The device with Alq_3 spacer has decreasing MR with increasing bias voltages, while the device without Alq_3 spacer shows opposite behavior. Most importantly, the introduction of Alq_3 spacer greatly enhanced the MR value. The MR value of the Fe/Alq_3/V[TCNE]$_x$/Al device is one order of magnitude larger than that of the Fe/V[TCNE]$_x$/Al device. For example, at 100 K and 500 mV, the former has a MR value of 0.34% while the latter only has 0.07%. The Alq_3 device also outperforms the rubrene device we reported before [17] which employed 10 nm rubrene as the spacer while other layers remained the same. The rubrene device had a maximum MR of 0.18% at 100 K, much smaller than that

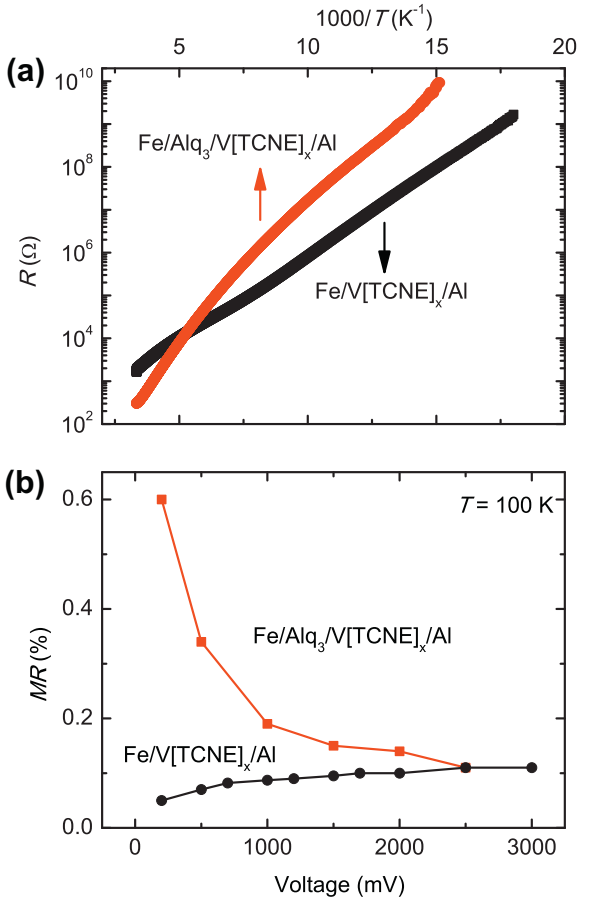

Fig. 6. (a) Device resistances as a function of temperature for Fe/V[TCNE]$_x$/Al (black) and Fe/Alq$_3$/V[TCNE]$_x$/Al (red). (b) Comparison of MR values at 100 K at different bias voltages. (For interpretation of the references to colour in this figure legend, the reader is referred to the web version of this article.)

of 0.6% obtained at 100 K from the Alq$_3$ device. We also noticed that the rubrene device showed higher current in the *I–V* plots, in part due to the high mobility of the rubrene film. However, the relation between the mobility of the spacer material and the MR is unclear.

5. Conclusions

We have fabricated and compared two types of device: Fe/V[TCNE]$_x$/Al and Fe/Alq$_3$/V[TCNE]$_x$/Al. We have shown that the device with Alq$_3$ spacer has better performance in terms of higher MR values. We also showed that the spacer layer is not indispensable for the spin vale to function. This would greatly simplify the deposition processes and significantly reduce the fabrication cost of the future organic spin valve applications.

Acknowledgements

This work was supported in part by AFOSR Grant No. FA9550–06-1–0175, DOE Grant Nos DE-FG02–01ER45931, DE-FG02–86ER45271, NSF Grant No. DMR-0805220, the Center for Emergent Materials (an NSF-MRSEC; Award Number DMR-0820414) at The Ohio State University and the Institute for Materials Research at The Ohio State University.

References

[1] S.A. Wolf, D.D. Awschalom, R.A. Buhrman, J.M. Daughton, S. von Molnár, M.L. Roukes, A.Y. Chtchelkanova, D.M. Treger, Science 294 (2001) 1488.
[2] W.J.M. Naber, S. Faez, W.G. van der Wiel, J. Phys. D Appl. Phys. 40 (2007) R205.
[3] V.A. Dediu, L.E. Hueso, I. Bergenti, C. Taliani, Nat. Mater. 8 (2009) 707.
[4] G. Szulczewski, S. Sanvito, M. Coey, Nat. Mater. 8 (2009) 693.
[5] Z.H. Xiong, D. Wu, Z. Valy Vardeny, J. Shi, Nature 427 (2004) 821.
[6] T.S. Santos, J.S. Lee, P. Migdal, I.C. Lekshmi, B. Satpati, J.S. Moodera, Phys. Rev. Lett. 98 (2007) 016601.
[7] H. Vinzelberg, J. Schumann, D. Elefant, R.B. Gangineni, J. Thomas, B. Buchner, J. Appl. Phys. 103 (2008) 093720.
[8] J.J.H.M. Schoonus, P.G.E. Lumens, W. Wagemans, J.T. Kohlhepp, P.A. Bobbert, H.J.M. Swagten, B. Koopmans, Phys. Rev. Lett. 103 (2009) 146601.
[9] C. Barraud, P. Seneor, R. Mattana, S. Fusil, K. Bouzehouane, C. Deranlot, P. Graziosi, L. Hueso, I. Bergenti, V. Dediu, F. Petroff, A. Fert, Nat. Phys. 6 (2010) 615.
[10] D. Sun, L. Yin, C. Sun, H. Guo, Z. Gai, X.-G. Zhang, T.Z. Ward, Z. Cheng, J. Shen, Phys. Rev. Lett. 104 (2010) 236602.
[11] J.H. Shim, K.V. Raman, Y.J. Park, T.S. Santos, G.X. Miao, B. Satpati, J.S. Moodera, Phys. Rev. Lett. 100 (2008) 226603.
[12] J.-W. Yoo, H.W. Jang, V.N. Prigodin, C. Kao, C.B. Eom, A.J. Epstein, Phys. Rev. B 80 (2009) 205207.
[13] J.-W. Yoo, C.-Y. Chen, H.W. Jang, C.W. Bark, V.N. Prigodin, C.B. Eom, A.J. Epstein, Nat. Mater. 9 (2010) 638.
[14] J.-W. Yoo, H. Jang, V. Prigodin, C. Kao, C. Eom, A. Epstein, Synth. Met. 160 (2010) 216.
[15] B. Li, J.-W. Yoo, C.-Y. Kao, H.W. Jang, C.-B. Eom, A.J. Epstein, Org. Electron. 11 (2010) 1149.
[16] B. Li, C.-Y. Kao, J.-W. Yoo, V.N. Prigodin, A.J. Epstein, Adv. Mater. 23 (2011) 3382.
[17] B. Li, C.-Y. Kao, Y. Lu, J.-W. Yoo, V.N. Prigodin, A.J. Epstein, Appl. Phys. Lett. 99 (2011) 153503.
[18] M. Gobbi, F. Golmar, R. Llopis, F. Casanova, L.E. Hueso, Adv. Mater. 23 (2011) 1609.
[19] R. Lin, F. Wang, M. Wohlgenannt, C. He, X. Zhai, Y. Suzuki, Synth. Met. 161 (2011) 553.
[20] G. Schmidt, D. Ferrand, L.W. Molenkamp, A.T. Filip, B.J. van Wees, Phys. Rev. B 62 (2000) R4790.
[21] J.S. Miller, A.J. Epstein, Angew. Chem. Int. Ed. Engl. 33 (1994) 385.
[22] J.M. Manriquez, G.T. Yee, R.S. McLean, A.J. Epstein, J.S. Miller, Science 252 (1991) 1415.
[23] V. Prigodin, N. Raju, K. Pokhodnya, J. Miller, A. Epstein, Adv. Mater. 14 (2002) 1230.
[24] K.I. Pokhodnya, A.J. Epstein, J.S. Miller, Adv. Mater. 12 (2000) 410.
[25] C.-Y. Kao, J.-W. Yoo, Y. Min, A.J. Epstein, ACS Appl. Mater. Interfaces 4 (2012) 137.
[26] D. Haskel, Z. Islam, J. Lang, C. Kmety, G. Srajer, K.I. Pokhodnya, A.J. Epstein, J.S. Miller, Phys. Rev. B 70 (2004) 054422.
[27] L. Fang, K.D. Bozdag, C.-Y. Chen, P.A. Truitt, A.J. Epstein, E. Johnston-Halperin, Phys. Rev. Lett. 106 (2011) 156602.
[28] J.J. Åkerman, R. Escudero, C. Leighton, S. Kim, D. Rabson, R.W. Dave, J. Slaughter, I.K. Schuller, J. Magn. Magn. Mater. 240 (2002) 86.
[29] N.P. Raju, T. Savrin, V.N. Prigodin, K.I. Pokhodnya, J.S. Miller, A.J. Epstein, J. Appl. Phys. 93 (2003) 6799.